Photoanode/Electrolyte Interface Stability in Aqueous Dye-Sensitized Solar Cells

Galliano, Simone; Bella, Federico; Gerbaldi, Claudio; Falco, Marisa; Viscardi, Guido; Grätzel, Michael; Barolo, Claudia. Photoanode/Electrolyte Interface Stability in Aqueous Dye-Sensitized Solar Cells. ENERGY TECHNOLOGY. 5 (2) pp: 300-311.
DOI: 10.1002/ente.201600285

Photoanode/Electrolyte Interface Stability in Aqueous Dye-Sensitized Solar Cells

Simone Galliano,[a] Federico Bella,*[b] Claudio Gerbaldi,[b] Marisa Falco,[a] Guido Viscardi,[b] Michael Grätzel,[c] and Claudia Barolo*[a]

[a] Prof. C. Barolo, M. Falco, S. Galliano, Prof. G. Viscardi
Department of Chemistry and NIS Interdepartmental Centre
Università degli Studi di Torino
Via Pietro Giuria 7, 10125 - Torino, Italy
E-mail: claudia.barolo@unito.it

[b] Dr. F. Bella, Prof. C. Gerbaldi
GAME Lab, CHENERGY Group, Department of Applied Science and Technology - DISAT
Politecnico di Torino
Corso Duca degli Abruzzi 24, 10129 - Torino, Italy
E-mail: federico.bella@polito.it

[c] Prof. M. Grätzel
Laboratory of Photonics and Interfaces, Institut des Sciences et Ingénierie Chimiques
Ecole Polytechnique Fédérale de Lausanne (EPFL)
Station 3, CH1015 - Lausanne, Switzerland

Abstract: O'Regan and Grätzel firstly conceived dye-sensitized solar cell (DSSC) to operate as artificial photosynthetic system able to convert solar light into electricity. Nevertheless, only very recently the scientific community is focusing on truly aqueous DSSCs, which use water as electrolyte, thus avoiding any flammable and toxic organic solvents. The most critical aspect of these devices is the photoanode/electrolyte interface. Indeed, it is necessary to select dyes capable of chemosorb onto the semiconductor layer concurrently allowing the aqueous electrolyte to impregnate the whole mesostructure of the electrode; at the same time, it is necessary to avoid the anchoring unit of the dye to be hydrolyzed by water, which causes the detachment of the sensitizer from the active material particles. This requires a thorough analysis of the structure/property relationships, particularly evaluating the chemical formula of the dyes and their stability and performances on the electrode surface in truly aqueous environment. Here we investigate nine different sensitizers, selected based on their different properties in terms of light absorption, chemical structure, hydrophobic/hydrophilic nature. Wettability, resistance to dye desorption and spectral variations of sensitized photoanodes, along with the photovoltaic performance of the resulting devices, are systematically investigated in order to identify some useful guidelines to choose and design suitable dyes of different colors for truly aqueous DSSCs.

Introduction

Dye-sensitized solar cells have recently exceeded 14% efficiencies,[1] but one of their main drawbacks still remains the use of a liquid electrolyte based on mixtures of highly volatile organic solvents.[2] High vapour pressure, severe environmental impact, toxicity and flammability are serious limiting factors of organic solvents, which in turn greatly affect the widespread diffusion of third-generation solar cells. Few interesting alternatives to organic solvents have been proposed, such as plastic crystals[3] and solid-state conductors,[4] which nevertheless are not at all cost-effective at present and demonstrate very limited long-term stability.[5] Moreover, an important aspect, often ignored, is still unsolved in standard aprotic DSSCs systems: the contamination by moisture/water. Such an undesired phenomenon influences the cell performance as well as its long-term stability.[6] Indeed, even if robust sealing systems encompassing specifically conceived barrier materials are utilised, traces of water, which are eventually introduced during cell assembly or upon standard operation under real ambient conditions, permeate/infiltrate the pores/voids of the semiconductor electrode film and contaminate the electrolytic solution.

In the last two decades, water has been considered a poisoner for DSSCs,[7] nonetheless the scientific community has recently focused great attention towards the study and development of water-based solar cells.[8] Indeed, aqueous DSSCs are non-flammable, cost-effective and environmentally friendly, and clearly they would not suffer from water contamination issues, with the added value that water may easily solvate many potential redox mediators.[9] Photoanode modifications,[10] introduction of novel additives and surfactants,[11] preparation of suitable cathodes[12] and stabilization of electrolytes[13] have progressively led to the fabrication of 100% aqueous DSSCs, and efficiencies close to 6% have recently been demonstrated at the laboratory scale.[14]

The most critical aspect in the field of aqueous DSSCs is represented by the photoanode/electrolyte interface. To date, the literature has proposed three different approaches to sensitize photoanodes and protect them in aqueous media. In the first one, traditional ruthenium-based organometallic dyes are used, and the hydrolysis of the carboxylic bond with the TiO_2 (with consequent dye detachment) is limited through the adoption of strongly acidic pH values for the aqueous electrolyte.[15] However, this approach is not successful for long periods; indeed, durability studies of these cells sealed with 100% aqueous electrolytes have never been reported. Recently, enhanced Ru-based dye-attachment to TiO_2 surfaces has been realized by coating molecularly functionalized surfaces with inorganic coatings by atomic layer deposition (ALD),[16] and the resulting devices demonstrated impressively enhanced stability.[17] However, ALD is rather expensive when compared to the low-cost techniques envisaged for aqueous DSSCs; moreover, to our knowledge an aging study of these ALD-coated electrodes in 100% aqueous electrolytes-based DSSCs has never been presented.

The second approach aims at using hydrophobic organic dyes, which are hardly detachable from the semiconductor active material particles. In some cases, this approach led to good results,[9a] but the high hydrophobicity of the photoanode has most often

prevented the penetration of the aqueous electrolyte in the cavities of the mesostructured photoelectrode, thus limiting the photocurrent generated by the cell. Nowadays, several research groups are focused on the synthesis of dyes molecules specifically designed (hydrophilic) to guarantee a good wettability of the photoelectrode, while concurrently bearing a water resistant (hydrophobic) TiO_2-binding group. Despite some of these dyes have been proposed in the last two years,[18] their stability is still insufficient and a proper trade-off between the hydrophilic and hydrophobic nature of the photoanode has not been identified so far.
Another controversial point in the literature regards the effective composition of the electrolyte, being very easy to get confused between water-based and truly aqueous DSSCs. Generally, water-based DSSCs are assembled with liquid electrolytes consisting of water / organic solvents mixtures at different ratios;[8b] on the contrary, in a truly aqueous device water is the only solvent in the electrolyte.[9a] As a result, it is rather difficult to compare properly the various devices presented in the literature in terms of performance and operational stability while using the same dye sensitizer, but different electrolyte compositions. In such a scenario, we firmly believe that, if the real aim is using water as the solvent for the redox mediator, it is necessary to move towards 100% organic solvents-free aqueous devices.
In this work, we propose a systematic study of the photoanode/electrolyte interface of truly aqueous DSSCs. This fundamental study compares nine different dye sensitizers, which reasonably represent the state of the art in the field of aqueous photovoltaics, *viz.* five commercial hydrophobic organic dyes (D35, D131, D205, D149, MK2), two slightly hydrophobic squaraine dyes prepared in our labs (VG10-C8, VG11-C2), two organometallic dyes with different hydrophilicity (N719, Z907). Wettability of the photoanodes, optical properties, eventual dye desorption phenomena, photovoltaic parameters and their stability over time are investigated, with the aim of identifying the most suitable dyes to be adopted by the scientific community in truly aqueous DSSCs.

Results and Discussion

1. Selection and chemisorption of dyes on TiO_2 photoanodes

With the aim of investigating the water resistance of photoanodes sensitized with different dyes, in this work nine different molecules (**Scheme 1**) have been selected and deeply studied. The selection criteria included the type of anchoring unit, the polarity of the molecular skeleton, the absorption region within the visible spectrum and the presence of metal centers. One-half of the dyes under study have recently been used in aqueous DSSCs, but quite often without any stability test (>500 h) to assure their effective resistance. In detail, N719 and Z907 were included because they are organometallic dyes having carboxyl groups as anchoring unit and a ruthenium-centered skeleton being polar (N719) or nonpolar (Z907). Three indolenine sensitizers (D131, D149 and D205) were selected on the basis of their different structural/coloring properties: i) D131 (yellow colored) has a cyanoacrylic anchoring group ; ii) D149 (purple) has a carboxyl anchoring group bound to a thiazolidine moiety; iii) D205 presents the same color and anchoring group of D149, but a long alkyl chain is connected to the thiazolidine moiety. As representative triphenylamine and carbazole dyes, D35 and MK2 were chosen. D35 is an orange dye bearing a triphenylamine skeleton with C4 chains and it is anchored to the TiO_2 electrode through a cyanoacrylic unit. MK2 (purple) is a carbazole dye with four thiophen-5-yl units and an acrylic anchoring group. Finally, two blue-greenish squaraine dyes (VG10-C8 and VG11-C2) have been selected for their symmetrical structure bearing two carboxyl anchoring groups.[19] VG10-C8 presents long alkyl chains (C8) on the indolenine nitrogen atoms, while VG11-C2 has two short (C2) ones and a malononitrile-modified squaric ring to block dye molecule in *cis*-conformational form.
Spectra of dye solutions and sensitized photoanodes are shown in **Figures S1-2** in the Supporting Information. Moreover, spectral features for each of the dyes are discussed in **Section S2** in the Supporting Information.

2. Resistance to dye desorption in aqueous environment

Dye desorption was periodically monitored during one week of immersion in water (10 mL) under dark condition to test the resistance of the sensitized electrodes to the aqueous environment, as detailed in the Experimental Section. Obviously, this volume of water is significantly larger than the amount of liquid electrolyte typically contained in a DSSC (≈0.004 mL), thus our experiment constitutes a sort of test of strength able to show how each dye can be considered as promising for being used in aqueous solar cells. For each photoelectrode, the intensity variation of the main absorption maxima was measured via UV-VIS spectroscopy (see **Figures S2-3** in the Supporting Information).
In the case of photoelectrodes sensitized with D149 and D205, the main absorption signals were saturated and the higher energy transition was considered as the reference for dye desorption estimation (**Table S2** in the Supporting Information). **Table S3** summarizes the averaged values of the main absorption maxima calculated for all the photoanodes sensitized with the same dye, at different dipping times.

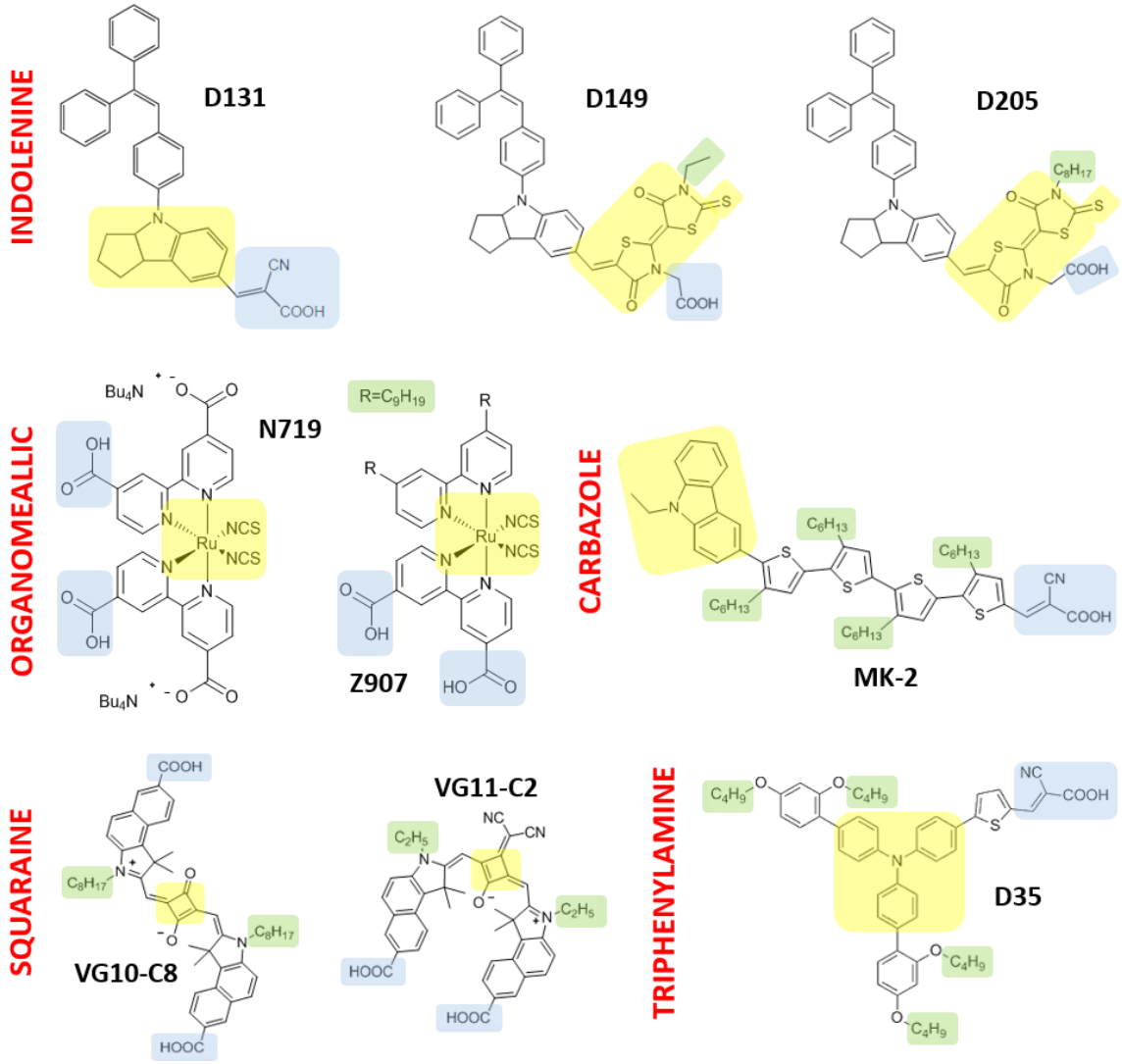

Scheme 1. Structural formulae of the sensitizer molecules investigated in the present work, which are typically employed in aqueous DSSCs. Color code: yellow for the main functional group, cyan for the anchoring unit, green for the lateral chains.

The main absorption maxima of N719, Z907 and VG11-C2 adsorbed on the photoanodes display a hypsochromic shift after dipping in water (**Table S3**). In the case of N719, a blue shift (about 30 nm in 2 h) of the lower energy absorption maximum is observed, together with the decrease of the signal intensity (–70% in 1 h) because of dye desorption. This result is consistent with literature data from Hahlin *et al.*,[20] who found that the blue shift is due to the displacement of the HOMO level towards higher binding energies. The same authors found that rearrangements involving –NCS ligand occurred in the case of TiO_2 samples loaded in a water added N719 bath. Furthermore, they found evidences of TBA^+ desorption from the surface of the titania active material particles. Agrell *et al.* observed a decrease of –NCS absorption in the IR range, and a blue shift of the lower energy peak in the VIS region after having dipped TiO_2 samples sensitized with N719 in an electrolyte solution added with 5% water.[21] These authors associated the blue shift in the VIS region to –NCS exchange with water, and found that this condition negatively affected the performance of the solar cell. Evidences of –NCS release as an effect of exchange with water or –OH groups was found by Lu *et al.* as well.[22]
The absorption maxima in the spectra of electrodes sensitized with Z907 during this test display a blue shift as well (**Table S3**). As the HOMO of this Ru-based dye is partly located on the thiocyanate ligands, the blue shift observed is likely due to –NCS exchange with water, just as in the case of N719. Moreover, in the case of Z907, the peak intensity at higher energy has increased (+35%), whereas the peak intensity at lower energy has decreased (–10%) over time (**Figure S11F** in the Supporting Information). Conversely, Hahlin *et al.* found that the hydrophobic chains of Z907 could prevent water from causing structural changes in the dye molecules loaded on TiO_2, and could not find any remarkable difference between the absorption spectra of the sample loaded in a water-added dye solution and the reference sample.[20] This incongruity may be due to lower contact time with lower amounts of water with respect to our experiment. Experimental data collected during our work show that N719 dye was completely desorbed from TiO_2 after 4 h of dipping, while Z907 dye remained stable, even if its desorption percentage is hardly quantified. Indeed, as stated above, the intensity of the two absorption peaks of Z907 shifted in opposite ways after permanence in water. Anyway, we did not detect the presence of Z907 in water, therefore the dye-electrode interaction can be considered as water-resistant. This evidence suggests that the long alkyl chains in Z907 are effective in preventing water from reaching the anchoring groups and desorbing the dye molecules.

The shift displayed in the case of VG11-C2 could be ascribed to the interaction of water with malononitrile moiety owing to –CN group polarity (**Table S3**). VG10-C8 squaraine does not display such behavior and, presumably, the long alkyl chains prevent such interactions. Alternatively, they may occur without affecting the absorption wavelengths, even though intermolecular interactions with water are reasonably expected to influence the dye vibrational motions and the previously discussed high-energy transitions in squaraines spectra, consequently.

Both squaraines were desorbed from the TiO_2 layer after being exposed to water (**Figure 1A-B**). A linear fit of the first 4 h of permanence in water allowed us to calculate the initial desorption rate (v_{des}^{i}), the values of which are shown in **Figure 1A-B**. Dye detachment was observed to occur fast (v_{des}^{i} = 0.05-0.20 h^{-1}) during the initial few contact hours and seemed to reach a plateau within the first week. Longer immersion times (over one week) would be required to assess whether a plateau value is reached or the dyes could be completely detached. According to the computational model by De Angelis *et al.*,[7a] desorption of squaraine dyes bound to anatase by bidentate linkages occurs after absorption of water on the semiconductor and starts by the detachment of one oxygen atom. After the first link break, the proton from the –COOH group adsorbed on the surface after dye chemisorption is extracted from the semiconductor surface and transferred to the carboxylate group. The dye is completely detached, thereafter.

The experimental data referred to samples loaded with the same squaraine show a large dispersion (**Figure 1A-B**). This fact was unexpected; nonetheless, we confirmed the poor reproducibility for squaraine dyes by reproducing the experiments weekly for one year. This particular feature is accompanied by the fact that in the literature about aqueous DSSCs no one presented green and blue dyes (like squaraines); therefore, some particular factor that is currently beyond our consideration is likely involved in the observed trend. Therefore, we have now started a more detailed study of green and blue dyes for aqueous DSSC in our laboratories trying to solve this issue.

Overall, VG10-C8 sensitized photoanodes demonstrated to be the most resistant to desorption, reaching in two cases a maximum detachment degree equal to 35%. On the other hand, short alkyl chains in VG11-C2 most likely play a key role in increasing the rate of dye detachment ($\bar{v}_{des}^{i}$ = 0.15 h^{-1} for VG11-C2, 0.06 h^{-1} for VG10-C8), allowing water molecules to reach the binding sites easily up to 100% dye detachment. Moreover, the release of physisorbed dye molecules may have given a higher contribution with respect to C8-substituted squaraines, as the formation of aggregates is more relevant in the case of sensitizers with short side chains. Desorption of CDCA (used in high quantities in the case of squaraine dyes) from the semiconductor surface may also be involved, as it would open channels towards the semiconductor surface.

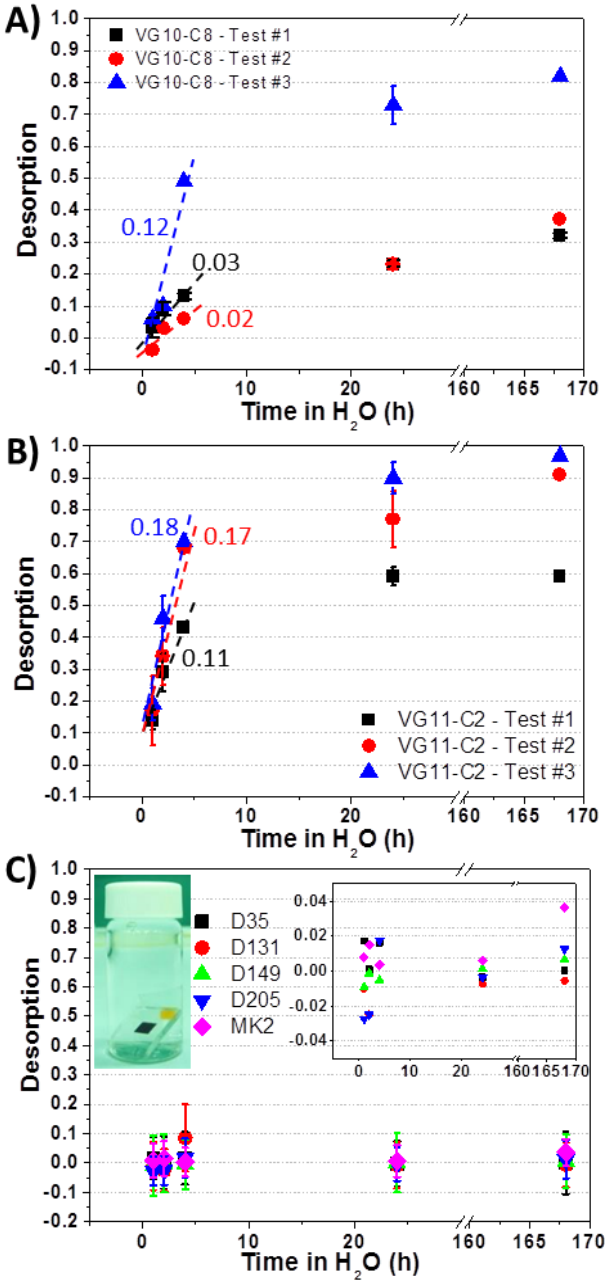

Figure 1. Desorption of squaraines (A-B) and hydrophobic organic dyes (C) versus immersion time in water. Error bars are referred to the propagated standard deviation (see also **Table S2** in the Supporting Information). Fitted initial desorption rate (in h^{-1}) for squaraine dyes are shown in panels A-B. *Insets* of plot C show the vial used during dye desorption test (where samples were dipped in ≈10 mL of deionized water) and a zoomed view of the data.

In the case of the two VG10-C8 sensitized samples, ≈65% of dye molecules could be retained on the semiconductor after one week of immersion in water (**Figure 1A**). This result is encouraging considering that, during this test, the samples were exposed to a much larger amount of water with respect to the real operational conditions of a DSSC, the photoanode of which usually faces a ≈50 μm-thick electrolyte layer. Overall, the synthesis of squaraine dyes containing longer chains and hydrophobic moieties capable of protecting the anchoring units from detachment will be necessary in order to apply this promising series NIR of dyes, with low-cost and tunable synthesis and exploit their potential in aqueous DSSCs. In fact, at the moment, no NIR absorbing dyes have been used in aqueous solar cells to the best of our knowledge.[8a,19]

3. Correlation between dye structure and photoanode wettability

Photoanode wettability represents a fundamental issue when the electrode/electrolyte interface is considered. In the present study, the apparent contact angle values settled generally in the range between 50 and 70° after one week of exposure to water. More in details, the apparent contact angles of the samples loaded with hydrophilic dyes were found to increase and reached a plateau within the initial 24 h. In the case of hydrophobic dyes, the reverse trend was observed, as the contact angle decreased over contact time. Noteworthy, samples sensitized with D35 still displayed a 70° (± 9) apparent contact angle after one week of immersion in water, which might be related to the absence of CDCA (that acts as a surfactant) in the immersion bath. In the case of D149, we observed a

peculiar behavior as well: the apparent contact angle dropped from 103° (± 2) to 48° (±2) after one hour of immersion in water and then slightly increased upon prolonged immersion times up to 68° (±5).

In the previous Section, we showed that photoanodes sensitized with hydrophobic organic dyes (D149, D205, D131, MK2, D35; see **Figure 1C**) did not display any shift in the absorption maxima, neither desorption after one week of immersion in water. Poor interaction with water provided by the hydrophobic organic dyes is consistent with the contact angle values measured just after dye uptake. All the samples sensitized with these dyes displayed contact angles exceeding 90°, which is the conventionally fixed value above which surfaces are considered unwettable by water.[23] The hydrophobicity of the sensitized photoanodes was found to increase in the following order (**Figure 2** and **Tables S2-3** in the Supporting Information):

N719 < VG11-C2 < VG10-C8 < D131 ≈ D149 < MK2 < Z907 < D35 ≈ D205

This trend is in line with the state of the art aqueous DSSCs, where the best long-term stability has been achieved while using MK2 and D-series dyes.[9a,10b]

On the other hand, N719 dye desorbed from the semiconductor layer in less than 2 h. This is quite reasonable considering its rather hydrophilic nature. Nonetheless, several research groups used this specific dye sensitizer in their aqueous DSSC. For example, Zhang *et al.* published a 3.96% efficiency for a 100% aqueous electrolyte cell, which was still operative (37% of the initial efficiency) after 50 days of aging at ambient temperature under 1 sun irradiation.[11b] We find this result much unexpected and markedly different from our present findings, where the N719 dye is completely desorbed after only few hours of immersion in water; moreover, Zhang *et al.* introduced an ionic surfactant in their aqueous electrolyte in order to increase the wettability of the photoanode surface. In our experiments, we clearly evidenced the water sensitivity of N719 dye, which may explain why several literature studies proposed this dye for aqueous DSSCs with no evidence of its long-term stability.[11a,24]

In the case of the reference (not sensitized) photoelectrodes, the contact angle was found to increase after the immersion step (**Table S4** in the Supporting Information). Indeed, the contact angle of bare (dry) TiO_2 was ≈35° and increased up to 51° after 17 h of dipping in EtOH (to mimic dye uptake conditions) and 24 h of immersion in water. This variation should be somewhat connected with water permeation inside the mesopores of the semiconductor layer, but also with surface adsorbed water molecules, since their adsorption onto the anatase surface is known to be energetically favored.[7a]

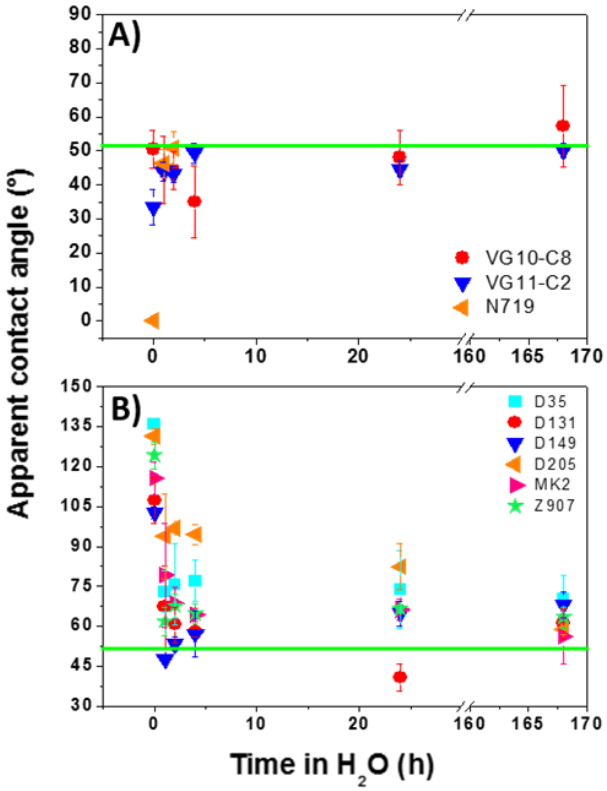

Figure 2. Average apparent contact angle values of samples sensitized with hydrophilic (A) and hydrophobic (B) dyes versus immersion time in water. Error bars refer to the standard deviations. The straight green line fixed at 51.4° corresponds to the apparent contact angle displayed by a sample of bare TiO_2 after 24 h of immersion in water.

Overall, the changes suggest that, under these experimental conditions, even hydrophobic dye molecules could not prevent water from infiltrating the semiconductor layer. Anyway, in the case of hydrophobic sensitizers, the local repulsive interactions at the dye/water interface may have hindered water diffusion near the anchoring groups, thus avoiding desorption.

After one week of exposure to water, some electrodes were dried in a desiccator for few days at ambient temperature. The apparent contact angles of the electrodes sensitized with hydrophobic dyes after dehydration showed a little increase (**Table S4** in the Supporting Information), but the results suggested that most part of the water adsorbed on TiO_2 or filling the pores could not be completely removed under these mild conditions.

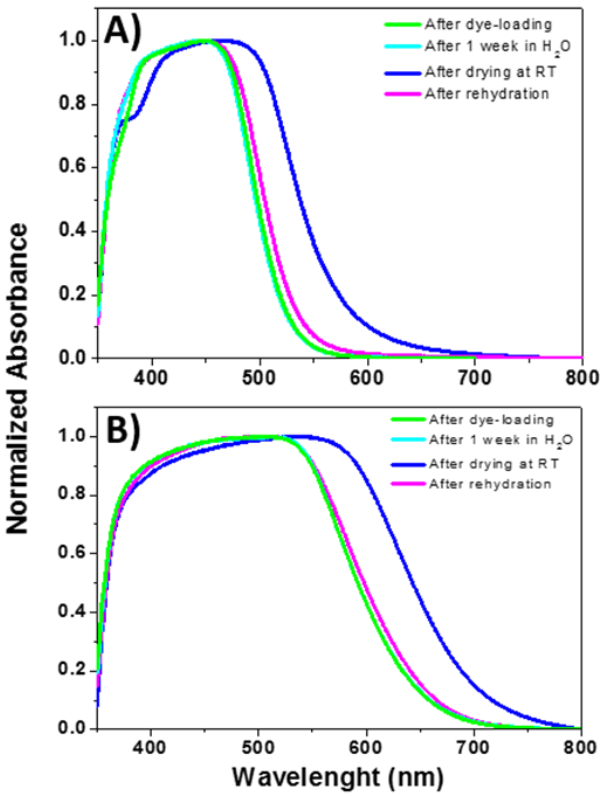

Figure 3. Absorption spectra of the photoanodes sensitized with D131 (A) and MK2 (B) dyes under different conditions.

The UV-VIS spectra of the dried electrodes sensitized with D131 as well as MK2 dyes displayed a sizeable bathochromic shift (about 15 and 25 nm, respectively, as shown in **Figure 3**). After rehydration upon few seconds of re-immersion in water, the samples displayed the same absorption wavelengths as in the spectra recorded right after dye loading. The observed solvatochromism is likely ascribable to the rearrangement of surface aggregates and/or to intermolecular interactions between sensitizer and water. The interaction between the surface adsorbed water and the anchoring group of D131 could likely result in such shift, as the cyanoacrylic moiety of this dye gives a strong contribution to the LUMO level. In the case of MK2, the formation of J-aggregates in the presence of water is consistent with recent literature reports.[25]

Overall, general guidelines may be obtained from the experiments of water resistance, UV-VIS spectroscopy and surface wettability. As regards the tested anchoring units, a preferable group seems not to exist, since both carboxylic and cianoacrylic moieties proved to be stable in water. Therefore, it can be stated that the discriminating factor for the stability in water of a sensitizer is given by the size of the hydrophobic molecular skeleton rather than by the anchoring group. Dyes stable in water must contain a bulky moieties possibly near the anchoring group of alkyl chains ($\geq$ C4) to avoid desorption from the semiconductor surface; therefore, as in the case of N719 and VG11-C2, water easily detaches dye molecules from TiO_2. Contact angle measurements also demonstrated that polar molecules-sensitized electrodes tended to increase their contact angle upon time up to ≈51° (value for pristine wetted TiO_2); on the contrary, apolar dyed photoanodes increased their wettability reaching a plateau value of contact angle slightly higher than 51° (i.e., in the range of 55-75°), that was not sufficient for detaching.

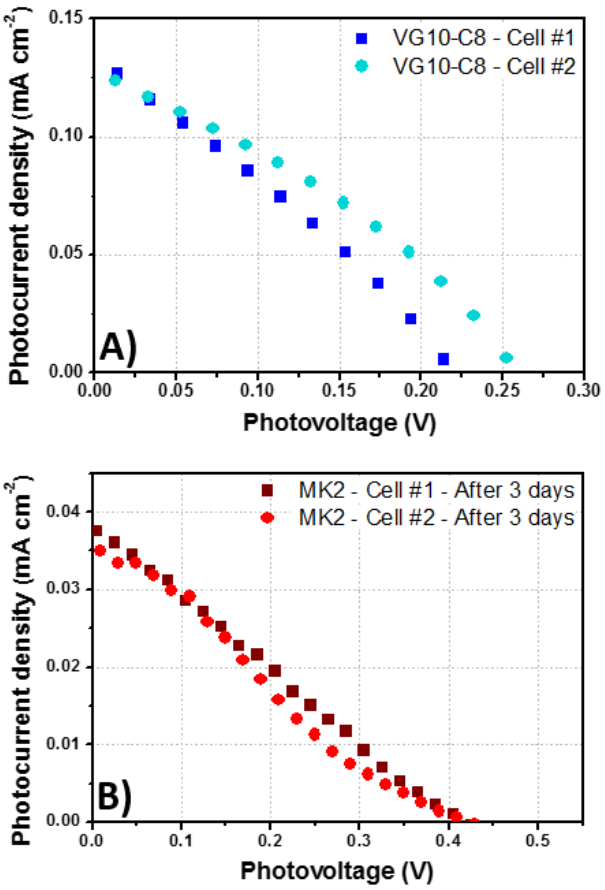

Figure 4. J-V curves (3rd run at 1 sun) of the cells sensitized with VG10-C8 (A) and MK2 (B). The electrolytes consist of NaI 0.50 M + I_2 25 mM in H_2O.

4. Photovoltaic performance of aqueous DSSCs

In the previous sections, good stability in aqueous environment was demonstrated for all of the chemisorbed dyes showed, with the exception of N719 and VG11-C2 that rapidly desorbed, and Z907 that remained bonded to TiO_2 but showed significant spectral variations. The photovoltaic performance of all the remaining dyes was tested in terms of photocurrent-photovoltage curves under 100 mW cm^{-2} illumination intensity.

Table 1. Photovoltaic parameters referred to J-V curves shown in **Figure 4**.

Cell	V_{oc} (mV)	J_{sc} (mA cm^{-2})	*FF*	*PCE* (%)
VG10-C8 Cell #1	214	0.14	0.29	0.009
VG10-C8 Cell #2	252	0.13	0.34	0.011
MK2 Cell #1	445	0.03	0.31	0.004

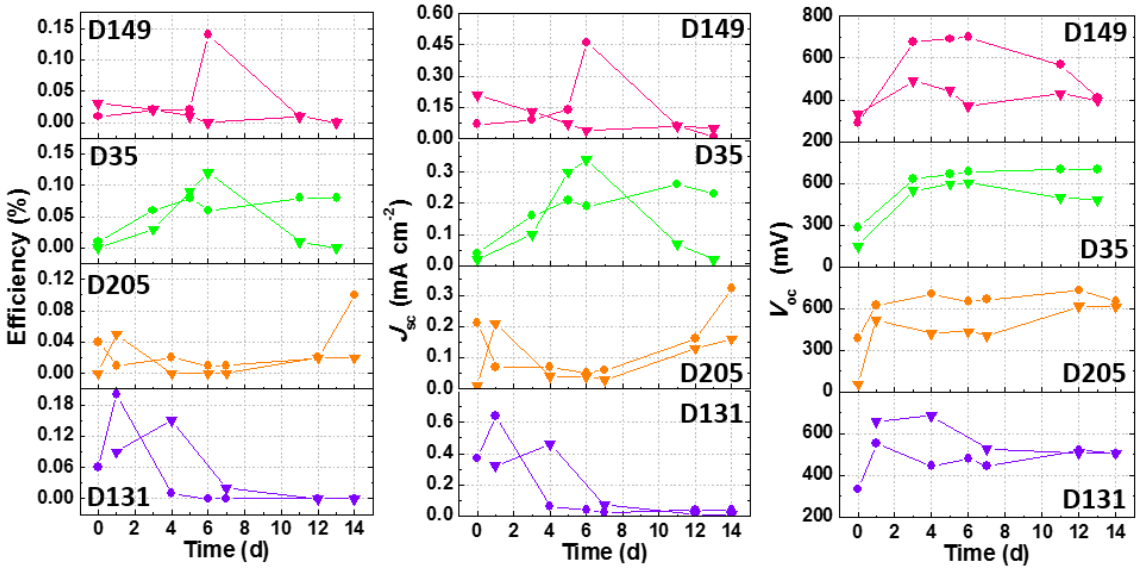

MK2 Cell #2	489	0.03	0.27	0.004

Figure 5. Photovoltaic parameters versus time for DSSCs (▼ cell #1, ● cell #2) filled with NaI 0.50 M + I_2 25 mM in H_2O and sensitized with different dyes. All data are referred to the last of three consecutive measurements at 1 sun.

In all the cases, poor photocurrent generation was obtained (see **Table S6** in the Supporting Information). The cells sensitized with VG10-C8 showed a low photocurrent signal (J_{sc} = 0.14 mA cm^{-2}) right after cell assembly (**Figure 4A** and **Table 1**). It is worth noting that these cells display a very low *FF*, resulting in a nearly linear photocurrent drop upon photovoltage increase. This evidence, together with the observed low V_{oc} values, suggests that both high recombination phenomena and high series resistance affect the photovoltaic performance of these cells. Low regeneration efficiency at the maximum power point might also account for such low *FF*.[26] Remarkably unstable systems were obtained in the case of MK2 dye under these experimental conditions. The J-V curves in **Figure 4B** were recorded few days after cell assembly. Efficiency data referred to previous and successive measurements are not shown here because of irregular shaped curves determining unreliable *FF* parameters. Very low photocurrent could be generated by the cells sensitized with MK2, and their V_{oc} decreased over time. In this case, dipping conditions were selected based on the article by Spiccia and co-workers,[27] which describes solar cells operating with a cobalt-based redox shuttle in aqueous medium. The authors reported relatively high J_{sc} values exceeding 8 mA cm^{-2}, even for devices where the amount of added poly(ethylene glycol) (PEG, as additive) was shown to hinder mass transport through the electrolyte solution. Moreover, they reported V_{oc} higher than 600 mV. Such improved values were attributed to lower recombination at the TiO_2/electrolyte interface and more efficient regeneration when compared to iodide/iodine-based systems. It is worth noting that these authors added 0.7 M *N*-methylbenzimidazole (NMBI) in the electrolyte solution. This benzimidazole compound is often used to improve V_{oc} as it interacts with the semiconductor, thus reducing dark current generation.[28] In our laboratories, several attempts were made to dissolve organic NMBI in iodide/iodine aqueous solutions; unfortunately, it was found to cause iodine precipitation, even at high NaI concentrations and in the presence of PEG-300, Tween-20 detergent or CDCA and alkylimidazolium iodide salts.

In **Figure 5** (see also **Table S6** in the Supporting Information) it is clear that the trends in *PCE* and J_{sc} are similar in the case of solar cells sensitized with D131, D205, D149 and D35. It is worth noting that, in most cases, J_{sc} values higher than 0.1 mA cm^{-2} were reached after several days. V_{oc} values ≈600 mV were achieved with these four dyes (**Figure 5**). It is worth stating that the two cells assembled with each sensitizer displayed V_{oc} values differing by 100 mV or more. The other photovoltaic parameters were probably too low to reflect such variability. Moreover, V_{oc} values varied over time. As the flat band potential (E_{fb}) is pH sensitive in aqueous medium, the release of surface adsorbed protons might give a contribution to the increase of V_{oc}, as it would result in the shift of E_{fb} towards more cathodic potential values.

The photovoltaic parameters resulting from the best performing cell are shown in **Table 2**. The highest efficiency value achieved during this experiment was 0.2%, with a J_{sc} = 0.64 mA cm^{-2} using D131 dye. This result is rather surprising, especially if one considers that D131 shows the narrowest VIS absorption (see **Figure S11B** in the Supporting Information); indeed, it is well known from the literature that red dyes (D149 and D205) show higher photocurrent (and efficiencies) if compared to yellow ones (D131). In the present case, the obtained outcome may be related with the fact that D131 sensitized photoanodes displayed the lowest contact angles together with D149. The shape of the J-V curves (**Figure 6**) corresponding to the best performances suggests an ongoing degradation, and for D131-sensitized cells this occurred in one week (**Figure 5**). The slope close to J_{sc} seems to point at current leakages. This might be ascribed to low DC resistance to charge transfer at the TCO/electrolyte interface at the bottom of the semiconductor layer (r_{BL}) or poor regeneration efficiency (φ_{reg}). To this purpose, Law *et al.* observed that a sizeable improvement of the photocurrent generated by water-based solar cells loaded with D149 dye resulted from adding large amounts of iodide salts to the electrolyte.[11a] The authors suggested that poor regeneration efficiency may have played a specific role in determining the value of the photocurrent at low iodide concentration. On the other hand, Leandri *et al.* found that oxidized D35 sensitized photoanodes could not be fully reduced by 2 M KI or 8 M guanidinium iodide (GuI) aqueous solutions by photo-induced absorption spectroscopy measurements, even though CDCA was co-adsorbed on the semiconductor.[12]

Table 2. Best photovoltaic performances (3rd run under 1 sun irradiation) of DSSCs assembled with aqueous electrolytes containing NaI 0.50 M + I_2 25 mM.

Cell	Day	V_{oc} (mV)	J_{sc} (mA cm^{-2})	*FF*	*PCE* (%)
D131	1	552	0.64	0.56	0.20
D205	14	649	0.32	0.50	0.10
D149	6	699	0.46	0.43	0.14
D35	6	604	0.34	0.58	0.12

From a thermodynamic point of view, dye regeneration is more favored in acetonitrile. The redox potential of the electrolyte solution used during this experiment, calculated according to the Nernst equation, is about 150 mV higher in water than in ACN (i.e., 0.52 V *vs.* NHE in H_2O and 0.34 *vs.* NHE in ACN). Comparing the literature data reporting the redox potentials of the dyes under study on nanostructured TiO_2 layers (**Figure 7** and **Table 3**), the driving force for the dye cation reduction by I^- species follows the order:

D131 < D205 ≈ D149 ~ D35 < MK2

This is consistent with the maximum J_{sc} data displayed by the cells experimented in this work. Anyway, it should be stressed that literature data refer to cyclic voltammetry (CV) experiments made using ACN-based supporting electrolytes; the redox potentials may differ from those in aqueous medium because of the different environment due to the presence of another solvent, which may influence dielectric constant, second order interact-

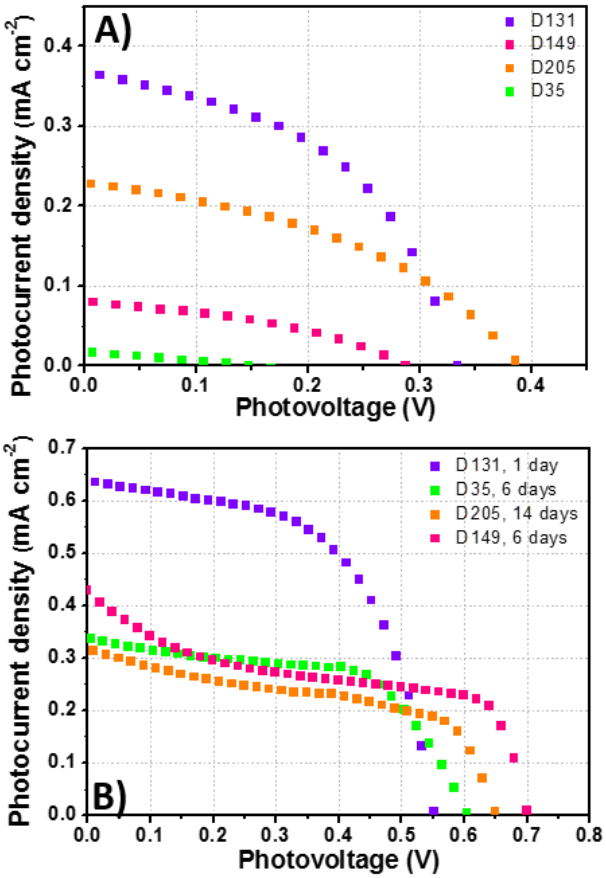

Figure 6. Panel A shows J-V curves (3rd measurement at 1 sun) of solar cells sensitized with D35, D149, D205 and D131 recorded just after cell assembly. The best J-V curves for each cell (filled with NaI 0.50 M + I_2 25 mM in H_2O) within the first 15 days of aging test are shown in panel B.

ons, etc. According to detailed analysis of the regeneration mechanism,[2a] the redox potential of the couple $I_2^{-\bullet}/I^-$ should be taken into account to evaluate the driving force for dye cation reduction. The standard potential of this redox couple in aqueous medium is 1.04 V *vs.* NHE, suggesting that, in the case of solar cells loaded with dye MK2, regeneration may not be energetically favored when compared to ACN-based electrolytes, where $E°(I_2^{-\bullet}/I^-)$ = 0.79 V. The indication that can be drawn from these experiments is that D131 dye is highly promising for aqueous DSSCs bearing the iodide/triiodide redox mediator, while MK2 dye becomes interesting in systems with cobalt-based electrolytes. While the latter has been recently proposed,[10a,27] it is rather surprising that no one has used D131 sensitizer in aqueous cells so far. Beside this, it must also be stated that the aqueous electrolyte used in this work has not been optimized, and its composition was selected after a preliminary screening with the only aim of evaluating the performance of cells sealed with different dyes, and not to obtain an efficiency and stability record (indeed, opaque electrodes and back-reflectors were not used). The investigation of the effect of the redox mediator (concentration and presence of additives) on cells efficiency and stability, along with electrolyte gelation into a quasi-solid matrix, represents the subject of a forthcoming article.

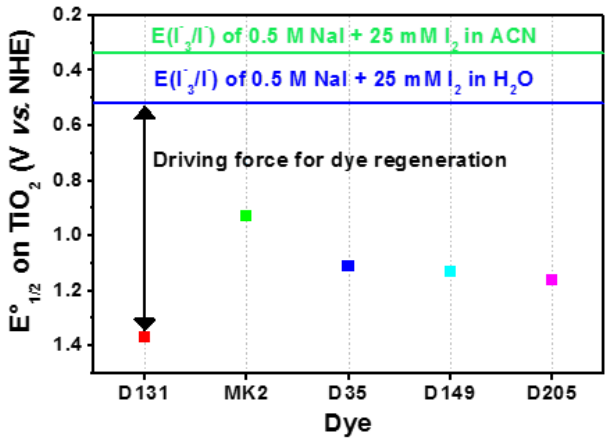

Figure 7. Midpoint redox potential on TiO_2 of the hydrophobic dyes under study extracted from literature data. The straight lines are fixed at the redox potentials of NaI 0.50 M + I_2 25 mM in H_2O (lower one) and ACN (upper one).

Table 3. List of the redox potentials of the hydrophobic dyes in ACN solution and on TiO_2 as resulting from the overall literature reports.

Dye	E_{ox} HOMO (V vs. NHE)	E_{red} LUMO (V vs. NHE)	$E^0_{1/2}$ (V *vs.* NHE)	
	Solution	Solution	Solution[a]	On TiO_2
D131	1.1[e]	−1.31[e]	1.21	1.37[f]
MK2	0.96[b]	−1.11[b]	1.04	0.93[c]
D35	1.04[h]	−1.37[h]	1.21	1.11[d]
D149	1.03[e]	−1.07[e]	1.05	1.13[f]
D205	0.98[g]	−1.1[g]	1.04	1.16[f]

[a] Midpoint redox potential calculated from data listed in the first two columns. [b] CV with 0.10 M $TBABF_5$ in ACN as supporting electrolyte.[29] [c] Calculated from data referred to CV measurements with 0.10 M $LiClO_4$ in ACN as supporting electrolyte.[30] [d] CV at 10 mV s^{-1} with 0.10 M $LiClO_4$ in MPN as supporting electrolyte.[31] [e] CV at 100 mV s^{-1} of a dye solution in ACN + 1.0 mM Fc + 0.10 M TBAP, tabulated assuming Fc^+/Fc = 0.63 V vs. NHE.[32] [f] CV with 0.10 M NBu_4PF_6 in ACN as supporting electrolyte, tabulated assuming Ag/AgCl (KCl 3.0 M) = 0.210 V vs. NHE.[33] [g] CV at 100 mV s^{-1} of a dye solution in DMF + 1.0 mM Fc + 0.10 M TBAP, tabulated assuming Fc^+/Fc = 0.63 V vs. NHE.[34] [h] CV at 100 mV s^{-1} of a dye solution in DMF + 50 mM $TBAPF_6$.[35]

Conclusions

In this work, spectral variations, resistance to dye desorption and wettability of TiO_2 photoanodes, loaded with nine different state of the art sensitizers and exposed to water, were systematically investigated by VIS adsorption analysis and contact angle measurements. These analysis allow to identify the relationship between the molecular structure and the stability in water of the sensitizer, besides some useful guidelines to select and design suitable dyes for truly aqueous DSSCs.

Contact angle measurements suggested a wettability variation of photoanode surface, but in different manner as function of the hydrophilicity/hydrophobicity ratio of the sensitizer molecules. Owing to immersion of sensitized photoanodes in aqueous electrolyte solution, water permeation inside the layer pores and surface adsorption occurred.

All the sensitizers showed moderate aggregation phenomena on the semiconductor film. J-, H-aggregates and π-π interactions led to bathochromic or hypsochromic shifts and peak broadening, which were correlated to the different molecular structures, according to the literature. Also the co-adsorption with CDCA could not completely suppress the aggregates formation for metal-free dyes.

Overall, the hydrophilic squaraine (VG11-C2) showed marked desorption phenomena in aqueous environment, while VG10-C8 dye was able to maintain ≈70% of the absorption signal after one week of immersion in water, probably thanks to the longer alkyl chains. Conversely, hydrophobic metal-free dyes (i.e., D35, D131, D149, D205 and MK2) did not desorb upon the experimental conditions adopted, even though contact angle measurements suggested that water could infiltrate the semiconductor mesopores over prolonged contact period. Concerning tested Ru-based sensitizers, opposite behaviors were observed: N719 dye desorbed very fast, while Z907 dye proved to be quite stable. Also in this case, such an effect is ascribable to the presence of long alkyl chains.

The repulsive interaction at the dye/water interface seems to be effective in preventing water from contacting the anchoring groups, anyway. On the other hand, if this hypothesis is correct, regeneration process might be negatively affected.

The photovoltaic performances of truly water-based lab-scale solar cells loaded with the more effective desorption-resistant dyes in aqueous solution and filled with a basic electrolyte containing NaI 0.50 M and I_2 25 mM were monitored over time. Overall, the photovoltaic performances of fresh cells were affected by low photocurrents, which – in a few cases – increased upon time reaching

the highest values after several days. All of the D-series dyes demonstrated to be promising for aqueous DSSCs and the fine-tuning of the redox mediator concentration along with the introduction of additives and jellifying agents will surely improve their efficiency and stability upon time. We can state that D131 is the highest performing dye, which also allows better photoanode wettability when compared to the other hydrophobic dyes. Moreover, from a thermodynamic viewpoint, regeneration of D131 molecules should be more favored if compared to the other dyes. In case of appropriate stabilization upon prolonged operation in real cell configuration, our opinion is that such a dye represents a strong candidate for future aqueous DSSCs, also due to its relatively narrow absorption in the visible spectrum that suggests its suitability for transparent building-integrated photovoltaics.

Experimental Section

1. Materials

Sodium iodide (NaI), iodine (I_2), chenodeoxycholic acid (CDCA), ethanol (EtOH), acetone (dimethyl ketone, DMK), *tert*-butanol (t-BuOH), toluene (Tol) and acetonitrile (ACN) were purchased from Sigma-Aldrich.

Sensitizers N719 (Ruthenizer 535 bis-TBA) and Z907 (Ruthenizer 520-DN) were purchased from Solaronix. MK2 dye was obtained from Sigma-Aldrich. D131, D205 and D149 sensitizers were purchased from Inabata Europe S.A. D35 (DN-F04) was obtained from Dyenamo AB. VG10-C8 and VG11-C2 dyes were synthesized in our laboratories accordingly to the synthetic procedure reported in ref. [36]. Chemical structures of all of these dyes are shown in **Scheme 1**, while their nomenclature and proton nuclear magnetic resonance (^{1}H-NMR, recorded on a Bruker Avance 200 NMR) are given in **Section S1** and **Figures S1-9** in the Supporting Information.

FTO-glass plates (sheet resistance 7 Ω sq^{-1}, purchased from Solaronix) were cut into 2 cm × 1.5 cm sheets and used as substrates for the fabrication of photoanodes and counter electrodes.

2. Fabrication of photoanodes and dipping conditions

The front electrodes were prepared by depositing a single layer of porous TiO_2 on the top of conductive substrates (previously cleaned with acetone and ethanol) using a screen printer equipment with a 43T mesh frame.[37] After deposition of the paste (18NR-T, Dyesol) and 20 min rest to allow an optimum relaxation, the TiO_2 layer was dried at 80 °C for 20 min and sintered by increasing the temperature up to 480 °C in 45 min. The fabricated transparent photoanodes (with a thickness of ≈6 μm and a covered area of 0.25 cm^2) were finally thermally activated at 450 °C for 20 min and, subsequently, soaked into a dye solution at 70 °C following the experimental conditions listed in **Table 4**. Dipping in the dye solutions was carried out at 22 °C under dark conditions and continuous shaking in a Buchi Syncore platform provided with a cooling plate. After dye loading, the photoanodes were rinsed in proper solvents to remove the residual dye not specifically adsorbed on the TiO_2 layer.

Table 4. Dye solutions and dipping conditions adopted for the investigation of the interfacial characteristics between photoanodes and aqueous electrolyte.

Dye	[Dye] (mM)	Solvent	[CDCA] (mM)	Dipping time (h)	Rinsing solvent
N719	0.3	EtOH	0	17	EtOH
Z907	0.2	EtOH	0	17	EtOH
D131	0.5	*t*-BuOH:ACN (1:1)	0.9	5	DMK
D205	0.5	*t*-BuOH:ACN (1:1)	0.9	5	DMK
D149	0.5	*t*-BuOH:ACN (1:1)	0.9	5	DMK
D35	0.5	EtOH	0	17	EtOH
MK2	0.3	*t*-BuOH:ACN:Tol (1:1:1)	0	6	EtOH
VG10-C8	0.01	EtOH	1.0	18	EtOH
VG11-C2	0.01	EtOH	1.0	15	EtOH

3. Investigation of the water effect on photoanodes

The evaluation of the water tolerance of photoanodes sensitized with different dyes was conducted via UV-VIS spectroscopy and contact angle measurements. The samples were dipped in ≈10 mL of deionized water MilliQ grade (γ = 72 mN m^{-1}) for periods ranging from 1 h to one week, under dark condition. The UV-VIS spectra and the contact angle measurements on the sensitized photoanodes were recorded after 0, 1, 2, 4, 24 and 168 h of dipping in deionized water. After being removed from water, the electrodes were dried by gently sandwiching them between two absorptive polypropylene sheets. The UV-VIS spectra were always recorded before the contact angle measurement.

For each photoanode, UV-VIS absorption spectra were recorded in the range between 350 and 700 nm on a CaryBio 300 spectrometer (Varian) and using a transparent electrode without sensitizer as the reference sample. In the case of dye desorption as an effect of dipping in water, the measurements were replicated by re-positioning the electrode two to three times, because surface inhomogeneity was found to determine sizeable variability connected to the sample placement. All the baselines were corrected subtracting the absorbance value at the highest wavelength (where absorbance should equal zero) to calculate desorption. Dye desorption was calculated by the following equation:

$$\overline{\mathrm{Des}}_{\mathrm{xh}} = 1 - \frac{\overline{\mathrm{Abs}_{\mathrm{xh}}}}{\overline{\mathrm{Abs}_{\mathrm{0h}}}} \quad \text{(Eq. 1)}$$

where $\overline{\mathrm{Des}_{\mathrm{xh}}}$ is the average value of dye desorption from the TiO_2 layer after *x* hours of immersion in water, $\overline{\mathrm{Abs}_{\mathrm{xh}}}$ is the average value of absorbance after *x* hours of immersion in water, $\overline{\mathrm{Abs}_{0\mathrm{h}}}$ is the average value of absorbance after rinsing. The propagated standard deviation $(\mathrm{sd}_{\mathrm{des\ xh}})$ associated with $\overline{\mathrm{Des}_{\mathrm{xh}}}$ was calculated by this equation:

$$\mathrm{sd}_{\mathrm{des\ xh}} = \left\{ \left[\frac{\overline{\mathrm{Abs}_{\mathrm{xh}}}}{\left(\overline{\mathrm{Abs}_{0\mathrm{h}}}\right)^2} \right]^2 \left(\mathrm{sd}_{\overline{\mathrm{Abs0h}}}\right)^2 + \left(-\frac{1}{\overline{\mathrm{Abs}_{0\mathrm{h}}}} \right)^2 \left(\mathrm{sd}_{\overline{\mathrm{Absxh}}}\right)^2 \right\}^{0.5} \quad \text{(Eq. 2)}$$

which follows from:

$$\mathrm{sd} = \sqrt{\sum_i \left(\frac{\partial f(x)}{\partial x_i}\right)^2 [\mathrm{sd}_i]^2} \qquad \text{(Eq. 3)}$$

where $\mathrm{sd}_{\overline{\mathrm{Abs0h}}}$ is the standard deviation associated with $\overline{\mathrm{Abs}_{0\mathrm{h}}}$ and $\mathrm{sd}_{\overline{\mathrm{Absxh}}}$ is the standard deviation associated with $\overline{\mathrm{Abs}_{\mathrm{xh}}}$.

The wettability of the sensitized photoanodes and its variation during the above said test was investigated by optical contact angle measurements on a DSA100 instrument (KRÜSS GmbH), equipped with a charge-coupled device camera and an automatic dosing system for the liquid. Deionized water MilliQ grade was used as the liquid for the analysis (droplet volume equal to 3 µL) using the sessile droplet method in static mode and under ambient conditions. Every drop was dispensed on a different area of the specimen, and each result was averaged on several measured drops, thus assuring a robust statistics. Images of the drops were elaborated by the DSA100 software using the Laplace-Young approximation, even though for such little volumes of liquid the effect of gravity could be safely neglected. Three photoanodes without sensitizer were dipped in absolute ethanol at 22 °C under dark conditions and used as the reference samples for contact angle measurements.

4. Fabrication and characterization of devices

The counter electrodes were cleaned in ethanol under stirring for 20 min and dried in air before cell assembly. They consisted in FTO conductive glasses platinized by spreading an H_2PtCl_6 solution on the plate surface followed by heating up to 400 °C for 30 min.

Photoanodes, after dipping and rinsing as reported in **Table 4**, were faced to the counter electrodes using 60 µm thick Surlyn thermoplastic frames (internal area 0.6 cm × 0.6 cm) as spacers.[38] All of these components were assembled by hot pressing at 110 °C for 20 s. The sandwich-type cell was subsequently filled with liquid electrolyte in a vacuum chamber. The electrolyte solution consisted of NaI 0.50 M and I_2 25 mM dissolved in ultrapure water (Milli-Q grade).

Current-potential (I-V) curves were measured using a Keithley 2440 Source-Measure Unit under AM 1.5G illumination (100 mW cm^{-2}) provided from a Newport 91195A class A solar simulator (calibrated through a Newport 91150V silicon reference solar cell).[39]

Acknowledgements

Dr. Claudio Magistris is gratefully acknowledged for ^{1}H-NMR measurements. C.B., S.G. and G.V. gratefully acknowledge financial support of the DSSCX project (PRIN 2010-2011, 20104XET32) from MIUR and the University of Torino (Ricerca Locale ex-60%, Bando 2015).

Keywords: aqueous electrolyte • dye-sensitized solar cell • water • stability • desorption

[1] K. Kakiage, Y. Aoyama, T. Yano, K. Oya, J. I. Fujisawa, M. Hanaya, *Chem. Commun.* **2015**, *51*, 15894-15897.

[2] a) A. Hagfeldt, G. Boschloo, L. Sun, L. Kloo, H. Pettersson, *Chem. Rev.* **2010**, *110*, 6595-6663; b) M. Grätzel, *J. Photochem. Photobiol., C* **2003**, *4*, 145-153.

[3] a) D. Xu, C. Shi, L. Wang, L. Qiu, F. Yan, *J. Mater. Chem. A* **2014**, *2*, 9803-9811; b) C. Shi, L. Qiu, X. Chen, H. Zhang, L. Wang, F. Yan, *ACS Appl. Mater. Interfaces* **2013**, *5*, 1453-1459.

[4] a) B. Xu, E. Gabrielsson, M. Safdari, M. Cheng, Y. Hua, H. Tian, J. M. Gardner, L. Kloo, L. Sun, *Adv. Energy Mater.* **2015**, *5*, art. no. 1402340; b) T. W. Jones, N. W. Duffy, G. J. Wilson, *J. Phys. Chem. C* **2015**, *119*, 11410-11418.

[5] a) B. Li, L. Wang, B. Kang, P. Wang, Y. Qiu, *Sol. Energy Mater. Sol. Cells* **2006**, *90*, 549-573; b) F. Bella, *Electrochim. Acta* **2015**, *175*, 151-161.

[6] B. Macht, M. Turrion, A. Barkschat, P. Salvador, K. Ellmer, H. Tributsch, *Sol. Energy Mater. Sol. Cells* **2002**, *73*, 163-173

[7] a) F. De Angelis, S. Fantacci, R. Gebauer, *J. Phys. Chem. Lett.* **2011**, *2*, 813-817; b) J. Weidmann, T. Dittrich, E. Konstantinova, I. Lauermann, I. Uhlendorf, F. Koch, *Sol. Energy Mater. Sol. Cells* **1999**, *56*, 153-165.

[8] a) F. Bella, C. Gerbaldi, C. Barolo, M. Grätzel, *Chem. Soc. Rev.* **2015**, *44*, 3431-3473; b) C. H. Law, S. C. Pathirana, X. Li, A. Y. Anderson, P. R. F. Barnes, A. Listorti, T. H. Ghaddar, B. O'Regan, *Adv. Mater.* **2010**, *22*, 4505-4509.

[9] a) H. Tian, E. Gabrielsson, P. W. Lohse, N. Vlachopoulos, L. Kloo, A. Hagfeldt, L. Sun, *Energy Environ. Sci.* **2012**, *5*, 9752-9755; b) T. Daeneke, Y. Uemura, N. W. Duffy, A. J. Mozer, N. Koumura, U. Bach, L. Spiccia, *Adv. Mater.* **2012**, *24*, 1222-1225.

[10] a) W. Xiang, D. Chen, R. A. Caruso, Y. B. Cheng, U. Bach, L. Spiccia, *ChemSusChem* **2015**, *8,* 3704-3711; b) C. Dong, W. Xiang, F. Huang, D. Fu, W. Huang, U. Bach, Y. B. Cheng, X. Li, L. Spiccia, *Angew. Chem. Int. Ed.* **2014**, *53*, 6933-6937.

[11] a) C. Law, O. Moudam, S. Villarroya-Lidon, B. C. O'Regan, *J. Mater. Chem.* **2012**, *22*, 23387-23394; b) H. Zhang, L. Qiu, D. Xu, W. Zhang, F. Yan, *J. Mater. Chem. A* **2014**, *2*, 2221-2226.

[12] V. Leandri, H. Ellis, E. Gabrielsson, L. Sun, G. Boschloo, A. Hagfeldt, *Phys. Chem. Chem. Phys.* **2014**, *16*, 19964-19971.

[13] S. J. Park, K. Yoo, J. Y. Kim, J. Y. Kim, D. W. Lee, B. Kim, H. Kim, J. H. Kim, J. Cho, M. J. Ko, *ACS Nano* **2013**, *7*, 4050-4056.

[14] R. Y. Y. Lin, F. L. Wu, C. T. Li, P. Y. Chen, K. C. Ho, J. T. Lin, *ChemSusChem* **2015**, *8*, 2503-2513.

[15] M. Kaneko, T. Nomura, C. Sasaki, *Macromol. Rapid Commun.* **2003**, *24*, 444-446.

[16] a) K. Hanson, M. D. Losego, B. Kalanyan, G. N. Parsons, T. J. Meyer, *Nano Lett.* **2013**, *13*, 4802-4809; b) M. D. Losego, K. Hanson, *Nano Energy* **2013**, *2*, 1067-1069.

[17] D. H. Kim, M. D. Losego, K. Hanson, L. Alibabaei, K. Lee, T. J. Meyer, G. N. Parsons, *Phys. Chem. Chem. Phys.* **2014**, *16*, 8615-8622.

[18] H. Choi, B. S. Jeong, K. Do, M. J. Ju, K. Song, J. Ko, *New J. Chem.* **2013**, *37*, 329-336.

[19] D. Saccone, S. Galliano, N. Barbero, P. Quagliotto, G. Viscardi, C. Barolo, *Polymethine Dyes in Hybrid Photovoltaics: a Structure-Properties Relationship*, under review.

[20] M. Hahlin, E. Johansson, R. Scholin, H. Siegbahn, H. Rensmo, *J. Phys. Chem. C* **2011**, *115*, 11996-12004.

[21] H. Agrell, J. Lindgrenb, A. Hagfeldt, *Sol. Energy* **2003**, *75*, 169-180.

[22] H. Lu, T. Shen, S. Huang, Y. Tung, T. Yang, *Sol. Energy Mater. Sol. Cells* **2011**, *95*, 1624-1629.

[23] R. Förch, H. Schönherr, A. T. A. Jenkins, *Surface Design: Applications in Bioscience and Nanotechnology*, Wiley-VCH, **2009**, 471.
[24] H. Saito, S. Uegusa, T. N. Murakami, N. Kawashima, T. Miyasaka, *Electrochemistry* **2004**, *72*, 310-316.
[25] A. Nepomnyashchii, B. Parkinson, *Langmuir* **2013**, *29*, 9362-9368.
[26] J. Jennings, Y. Liu, Q. Wang, *J. Phys. Chem. C* **2011**, *115*, 15109-15120.
[27] W. Xiang, F. Huang, Y. Cheng, U. Bach, L. Spiccia, *Energy Environ. Sci.* **2013**, *6*, 121-127.
[28] H. Yang, J. Liu, Y. Lin, J. Zhang, X. Zhou, *Electrochim. Acta* **2011**, *56*, 6271-6276.
[29] A. Kumari, I. Mondal, U. Pal, *New J. Chem.* **2015**, *39*, 713-720.
[30] Z. Wang, N. Koumura, Y. Cui, M. Takahashi, H. Sekiguchi, A. Mori, T. Kubo, A. Furube, K. Hara, *Chem. Mater.* **2008**, *20*, 3993-4003.
[31] L. Yang, U. Cappel, E. Unger, M. Karlsson, K. Karlsson, E. Gabrielsson, L. Sun, G. Boschloo, A. Hagfeldt, E. M. J. Johansson, *Phys. Chem. Chem. Phys.* **2012**, *14*, 779-789.
[32] M. Matsui, M. Kotani, Y. Kubota, K. Funabiki, J. Jin, T. Yoshida, S. Higashijima, H. Miura, *Dyes Pigm.* **2011**, *91*, 145-152.
[33] A. Fattori, L. Peter, H. Wang, H. Miura, F. Marken, *J. Phys. Chem. C* **2010**, *114*, 11822-11828.
[34] S. Higashijima, Y. Inoue, H. Miura, Y. Kubota, K. Funabiki, T. Yoshida, M. Matsui, *RSC Adv.* **2012**, *2*, 2721-2724.
[35] D. Hagberg, X. Jiang, E. Gabrielsson, M. Linder, T. Marinado, T. Brinck, A. Hagfeldt, L. Sun, *J. Mater. Chem.* **2009**, *19*, 7232-7238.
[36] a) J. Park, N. Barbero, J. Yoon, E. Dell'Orto, S. Galliano, R. Borrelli, J. H. Yum, D. Di Censo, M. Grätzel, M. K. Nazeeruddin, C. Barolo, G. Viscardi, *Phys. Chem. Chem. Phys.* **2014**, *16*, 24173-24177; b) N. Barbero, C. Magistris, J. Park, D. Saccone, P. Quagliotto, R. Buscaino, C. Medana, C. Barolo, G. Viscardi, *Org. Lett.* **2015**, *17*, 3306-3309.
[37] a) F. Bella, N. Vlachopoulos, K. Nonomura, S. M. Zakeeruddin, M. Grätzel, C. Gerbaldi, A. Hagfeldt, *Chem. Commun.* **2015**, *51*, 16308-16311; b) F. Bella, A. Sacco, G. Massaglia, A. Chiodoni, C. F. Pirri, M. Quaglio, *Nanoscale* **2015**, *7*, 12010-12017.
[38] R. Tagliaferro, D. Gentilini, S. Mastroianni, A. Zampetti, A. Gagliardi, T. M. Brown, A. Reale, A. Di Carlo, *RSC Adv.* **2013**, *3*, 20273-20280.
[39] a) Y. I. Kang, J. H. Moon, *ChemSusChem* **2015**, *8*, 3799-3804; b) M. P. Antony, T. Moehl, M. Wielopolski, J. E. Moser, S. Nair, Y. J. Yu, J. H. Kim, K. Y. Kay, Y. S. Jung, K. B. Yoon, C. Grätzel, S. M. Zakeeruddin, M. Grätzel, *ChemSusChem* **2015**, *8*, 3859-3868; c) Z. He, J. Liu, S. Y. Khoo, T. T. Y. Tan, *ChemSusChem* **2016**, *9*, 172-176.